Available online at www.sciencedirect.com
SCIENCE DIRECT®
Biochimica et Biophysica Acta 1660 (2004) 66–74
BIOCHIMICA ET BIOPHYSICA ACTA
BBA
www.bba-direct.com

Glutamate 87 is important for menaquinol binding in DmsC of the DMSO reductase (DmsABC) from *Escherichia coli*

Paulina Geijer[1], Joel H. Weiner*

CIHR Membrane Protein Research Group, Department of Biochemistry, 474 Medical Sciences Building, University of Alberta, Edmonton, Alberta, Canada T6G 2H7

Received 30 July 2003; received in revised form 22 October 2003; accepted 27 October 2003

Abstract

Escherichia coli dimethylsulfoxide (DMSO) reductase is a trimeric enzyme with a catalytic dimer (DmsAB) and an integral membrane anchor (DmsC). Using site-directed mutagenesis, we examined six residues in the periplasmic loop between helices two and three, potentially involved in menaquinol binding in DmsC. Mutants were characterised for growth, enzyme expression and activity, and 2-*n*-heptyl-4-hydroxoquinoline *N*-oxide (HOQNO) inhibitor binding. Mutations of leucine 66, glycine 67, arginine 71, phenylalanine 73 and serine 75 had no effect on menaquinol binding. Only a glutamate residue (E87) located in helix three was important for menaquinol binding. E87 was replaced with lysine, glutamine and aspartate. All three mutants were assembled into the membrane. Neither the lysine nor the glutamine mutant enzymes were able to support anaerobic growth on glycerol/DMSO minimal media or oxidise lapachol. The glutamine mutant bound the inhibitor with lower affinity compared to wild-type, whereas in the lysine mutant, binding was almost abolished. The aspartate mutant behaved as a wild-type enzyme. The data shows that E87 is important for menaquinol binding and oxidation and is likely to act as a proton acceptor in the menaquinol binding site.

Keywords: Dimethylsulfoxide; Quinol binding; Menaquinol; Anaerobic respiration; Membrane protein; Molybdopterin guanine dinucleotide

1. Introduction

Escherichia coli can grow on dimethylsulfoxide (DMSO) as a terminal electron acceptor by utilising DMSO reductase [1]. DMSO reductase is constitutively expressed during anaerobic growth on fumarate as a terminal electron acceptor but repressed by nitrate. The enzyme is encoded by the *dms*-operon located on the *E. coli* chromosome at approximately 20 min [2]. The *dms*-operon has been cloned and sequenced and the enzyme expressed to high levels [3]. DMSO reductase can utilise a wide variety of *S*- and *N*-oxides such as DMSO, TMAO, pyridine *N*-oxide and methionine sulfoxide [4].

DMSO reductase is a trimeric enzyme localised to the cytoplasmic membrane, with two extrinsic subunits and one membrane anchor. DmsA is the catalytic subunit with a molecular weight of 85.8 kDa. In the catalytic site, there is one molybdenum atom coordinated by two molybdopterin-guanosine dinucleotides (Mo-bisMGD) [5,6]. DmsB is a 22.7 kDa electron transferring subunit with four [4Fe–4S] iron–sulfur clusters organised in two ferredoxin-like motifs as judged by the amino acid sequence of DmsB. The midpoint potentials of the iron–sulfur clusters are −50, −120, −240, and −330 mV [7,8]. The −50 mV cluster is close to the menaquinol binding site [8,9] and the −120 mV cluster interacts magnetically with the Mo-bisMGD cofactor in DmsA [10]. The remaining two clusters may not be directly involved in electron transfer but may play a structural role. DmsC is a 30.8 kDa menaquinol oxidising subunit with eight transmembrane helices and the N- and

Abbreviations: Amp, ampicillin; BV, benzyl viologen; DMSO, dimethylsulfoxide; HOQNO, 2-*n*-heptyl-4-hydroxoquinoline *N*-oxide; Kn, kanamycin; $LPCH_2$, reduced lapachol; MGD, molybdopterin guanosine dinucleotide; PMSF, phenylmethanesulfonyl fluoride; Sm, streptomycin; Tet, tetracycline; TMAO, trimethylamine *N*-oxide

* Corresponding author. Tel.: +1-780-492-9723; fax: +1-780-492 0886.
E-mail addresses: paulina.geijer@biokem.lu.se (P. Geijer), joel.weiner@ualberta.ca (J. H. Weiner).
[1] Present address: Department of Biochemistry, Kemicentrum, Lund University, P.O. Box 124, S-221 00 Lund, Sweden. Tel.: +46-46-222-1401; fax: +46-46-222-4534.

0005-2736/$ - see front matter © 2003 Elsevier B.V. All rights reserved.
doi:10.1016/j.bbamem.2003.10.016

C-termini located on the periplasmic side of the cell membrane [11,12].

Only one menaquinol binding site has been identified in DmsC using 2-*n*-heptyl-4-hydroxoquinoline *N*-oxide (HOQNO) inhibitor binding studies [9]. With the proposed topology of DmsC, the menaquinol binding site is located close to the periplasmic side of the cell membrane [12]. One residue, DmsC–His65, has been identified as important for menaquinol binding [8,9]. When the histidine is mutated to an arginine, the enzyme loses the ability to oxidise menaquinol or bind the menaquinol analogue HOQNO.

We have investigated the effect on growth and quinol oxidation of mutations in the periplasmic loop between helices two and three and in glutamate 87 of DmsC (Fig. 1). The E87-residue is located in the periplasmic part of helix three (Fig. 1A). The residues are conserved in DmsC sequences in *Salmonella typhimurium*, *Haemophilus influenzae*, *Yersinia pestis* and in the YnfH protein in *E. coli* (Fig. 1B). We found that the carboxyl-group of glutamate 87 is important for menaquinol oxidation. The substitution of a positively charged residue abolishes the ability of mutant enzyme to support anaerobic growth on glycerol/DMSO minimal media. The glutamate residue is most likely a proton acceptor in the menaquinol binding site in DmsC.

2. Materials and methods

2.1. Strains and plasmids

The *E. coli* strains used in this study are TG1 ((K12, Δ(*lac-proAB*), *supE*, *thi*, *hsd* Δ5 F′ [*traD*36 *proA*$^+$*B*$^+$*lacI*^{q} *lacZ* ΔM15]), Amersham Biosciences), HB101 ((*supE*44, *hsdS*20 (r_B^- r_M^-) *recAB*, *ara*-14, *proA*2, *lacY*1, *galK*2, Sm^r, *xyl*-5 *mtl*-1), lab collection) and DSS301 ((TG1, Km^r, Δ*dmsABC*), lab collection [11]). TG1 was used for molecular cloning. All cloning procedures were performed with standard methods as described in Sambrook and Russel [13].

The plasmids used were pBR322 (Amp^R, Tet^R, Pharmacia), pTZ18R (Amp^R, *lacZ*, Pharmacia) and pDMS160 (pBR322, (*dmsABC*)$^+$, [14]). Site-directed mutants were produced with the QuickChange Site-Directed Mutagenesis kit (Stratagene, La Jolla, CA) with pEPK100 (pTZ18R, Sac1/Sal1-fragment of pDMS160 containing *dmsC*, this study), as the vector. All mutants were verified with DNA sequencing (DNA core facility, University of Alberta). After sequencing, the mutagenised *dmsC* fragments were subcloned from the high copy number mutant plasmids into pDMS160 for expression and enzyme studies.

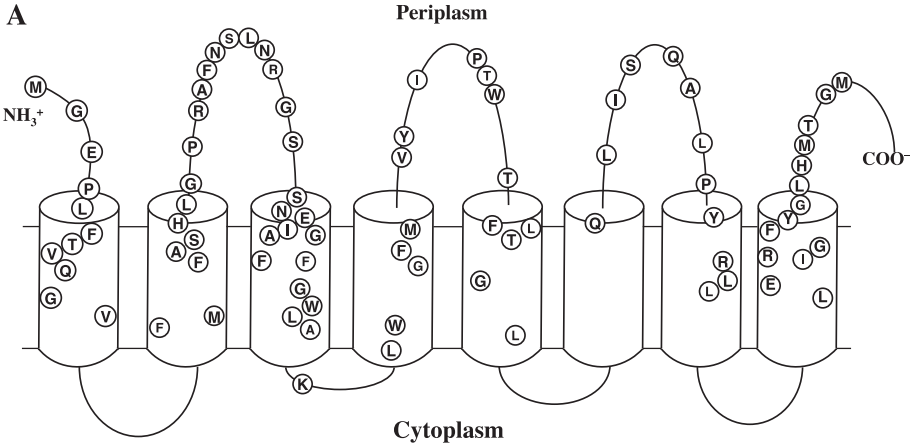

B

```
Ecoli       61 ASMLHLGSPMRAFNSLNRVGASALSNEIASGSIFF 95
Styphi2     61 ASMLHLGSPMRAFNSLNRVGASALSNEIASGSVFF 95
Ypestis     61 ASTLHLGSPMRAFNSLNRIGESALSNEIAAGSLFF 95
YnfH_Ecoli  60 ASVMHLGSPLRAFNSLNRIGASGLSNEIAAGSIFF 94
Styphi1     61 ASIMHLGSPMRAFNSLNRVGASALSNEIAAGSVFF 95
Hinfl       60 ASIMHLGLPIRAFNSLNRVGSSMMSNEIAAGAIFF 94
               ** :*** *:********:* * :*****:*::**
```

Fig. 1. Topology and protein alignment of DmsC. (A) A cartoon of the proposed topology and orientation of DmsC from *E. coli*. Circled residues represent absolutely conserved residues when six different DmsC sequences from *E. coli*: DmsC (P18777) and YnfH (P76173); *S. typhimurium*: DmsC-1 (Q8XEU5) and DmsC-2 (Q8Z6Y6); *Y. pestis*: DmsC (Q9X6B4) and *H. influenzae*: DmsC (P45002) are compared. (B) Sequence alignment of the periplasmic loop between helices two and three for the six DmsC like sequences in (A). The arrows indicate the residues discussed in this work.

2.2. Growth of bacteria

Cells were grown anaerobically at 37 °C on glycerol/DMSO minimal media or glycerol/fumarate minimal media [5]. Growth studies were set up in 125 ml flasks fitted with a side arm and filled to the top. Cell turbidity was monitored with a Klett-Summerson spectrophotometer equipped with a red filter (no. 66). Cells for preparation of membranes were grown on glycerol/fumarate minimal media for 48 h (HB101) or 24 h (DSS301) in 19 l cultures [8]. One percent overnight cultures in Luria–Bertani medium were used as inocula. Ampicillin (100 μg/ml) was regularly used in all cultures. Streptomycin (100 μg/ml) and kanamycin (40 μg/ml) were added to overnight cultures of HB101 and DSS301, respectively.

2.3. Preparation of membranes

Membranes were prepared by French press lysis as previously described [5,7]. The buffer used during the preparation contained 100 mM MOPS/KOH and 5 mM EDTA, pH = 7. A final concentration of 1 mM dithiothreitol was added before use. Prior to cell lysis a final concentration of 2 mM phenylmethanesulfonyl fluoride (PMSF) was added. Membranes were pelleted twice by centrifugation in a Beckman 50.2 Ti-rotor at 150,000 × *g* for 60 min. Before the second spin, PMSF was added to a final concentration of 2 mM. After a final resuspension in an appropriate volume, membranes were divided into aliquots and flash-frozen in N_2 (*l*). Protein concentrations were determined with a modified Lowry assay containing 1% (w/v) SDS.

2.4. SDS-PAGE and immunodetection with DmsA and DmsB antibodies

SDS-PAGE gels (12%) were run in the Laemmli buffer system [15] and stained with Coomassie brilliant blue. Samples were solubilised in Laemmli solubilisation buffer for 5–10 min at room temperature before loading onto the gels. For immunodetection, protein was transferred to nitrocellulose membranes and incubated with polyclonal DmsA and DmsB antibodies [16]. Protein bands were visualised using goat–anti rabbit antibody conjugated with horseradish peroxidase (BioRad Laboratories) and the ECL detection system (Amersham Pharmacia Biotech).

2.5. TMAO reduction assays

Benzyl viologen (BV)- and lapachol ($LPCH_2$)-mediated TMAO reduction was measured with 70 mM TMAO as the electron acceptor in MOPS buffer at pH = 7. The BV assay was previously described in Refs. [5,7]. Deaerated 50 mM MOPS was used as media. BV, Na-dithionite and TMAO were added to final concentrations of 0.2, 0.5 and 70 mM, respectively. After recording a stable baseline at 570 nm, membranes were added at an appropriate dilution. The extinction coefficient was 7.4 $mmol^{-1}$ cm^{-1} [17]. The $LPCH_2$ assay was previously described by Rothery et al. [18]. $LPCH_2$ oxidation is measured semi-anaerobically in stoppered cuvettes with a buffer containing 100 mM MOPS and 70 mM TMAO at pH = 7. $LPCH_2$ was added through the teflon stopper to a final concentration of 0.15 mM to record a baseline prior to adding membranes at appropriate dilution. $LPCH_2$ oxidation was recorded at 481 nm and the extinction coefficient is 2.66 $mmol^{-1}$ cm^{-1} [18]. A 10 mM stock solution in ethanol of reduced $LPCH_2$ was used for activity measurements. K_m values for $LPCH_2$ were estimated by measuring the activities at nine different $LPCH_2$ concentrations. The stock solution of $LPCH_2$ for K_m measurements was 20 mM in ethanol. The resulting data was fitted with the Briggs–Haldane equation to estimate the K_m value for $LPCH_2$ binding. The specific activities for the BV and $LPCH_2$ assays are the average of three measurements given in μmol e^- min^{-1} mg $protein^{-1}$.

2.6. Preparation of fluorescent molybdopterin derivative (Form A)

The method is described by Johnson and Rajagopalan [19]. Membranes prepared from HB101 cells were diluted with water prior to acidification and mixed with iodine to produce Form A of the molybdopterin cofactor. Ten milligrams of protein was used from each sample. Small aliquots were added to 1 M NH_4Cl before recording the spectra on a Perkin-Elmer LS-50B luminescence spectrometer. The excitation spectra and emission spectra were recorded from 240–420 to 410–520 nm, respectively. The emission wavelength was 442 nm and the excitation wavelength was 395 nm. The relative amount of Mo-bisMGD was determined by comparing the fluorescence peak height after subtraction of the fluorescence background from the chromosomal-encoded Mo-bisMGD-containing enzymes.

2.7. Fluorescence-quench titration of HOQNO

Binding of HOQNO to DmsC was measured by the quenching of HOQNO fluorescence and was performed according to van Ark and Berden [20]. HOQNO was added from a 0.12 mM stock in ethanol in 2 μl aliquots. Fluorescence was recorded at an excitation wavelength of 341 nm and an emission wavelength of 479 nm. The quenching was assayed at 0.25, 0.5, 0.75 and 1.0 mg protein ml^{-1}. The binding site concentration and dissociation constant of HOQNO were estimated by fitting the data according to Okun et al. [21]. The K_d is the average of the K_d values determined at each protein concentration.

3. Results

3.1. Mutagenesis of residues in the loop between helix two and three

Site-directed mutations in five different conserved residues were introduced in the periplasmic loop between helix two and three of DmsC (marked with arrows in Fig. 1B). Two mutated residues, L66D and G67A, are close to H65, which is known to be important for menaquinol binding and oxidation [8,9]. Three other mutations were introduced in the periplasmic loop after H65. The mutations were R71S, F73D, and S75C. All five residues studied are conserved between the six DmsC homologues in *E. coli*, *Y. pestis*, *H. influenzae*, *S. typhimurium* (DmsC-1 and DmsC-2), and YnfH of *E. coli* (Fig. 1B). The mutated *dmsC* genes were incorporated into the multicopy plasmid pDMS160 in place of the wild-type *dmsC* gene.

All mutant *dmsC* genes complemented growth on anaerobic glycerol/DMSO media in DSS301 (Δ*dms*) and did not interfere with growth in HB101. In DSS301, the doubling time for cells harboring plasmids pDMS160$^{DmsC\text{-}L66D}$, pDMS160$^{DmsC\text{-}G67A}$, pDMS160$^{DmsC\text{-}R71S}$, pDMS160$^{DmsC\text{-}F73D}$ and pDMS160$^{DmsC\text{-}S75C}$ mutants were 4.0, 3.8, 4.9, 4.9, and 4.9 h, respectively, compared to 4.1 h for the wild-type pDMS160. In HB101, the doubling times were 7.3, 5.9, 5.4, 6.0, and 6.8 h, respectively, for cells harboring the mutant plasmids compared to 6.7 h for the wild-type pDMS160. Thus, the cell growth doubling times for DSS301 and HB101 complemented with mutant DMSO reductase were similar to the doubling time for overexpressed wild-type DMSO reductase.

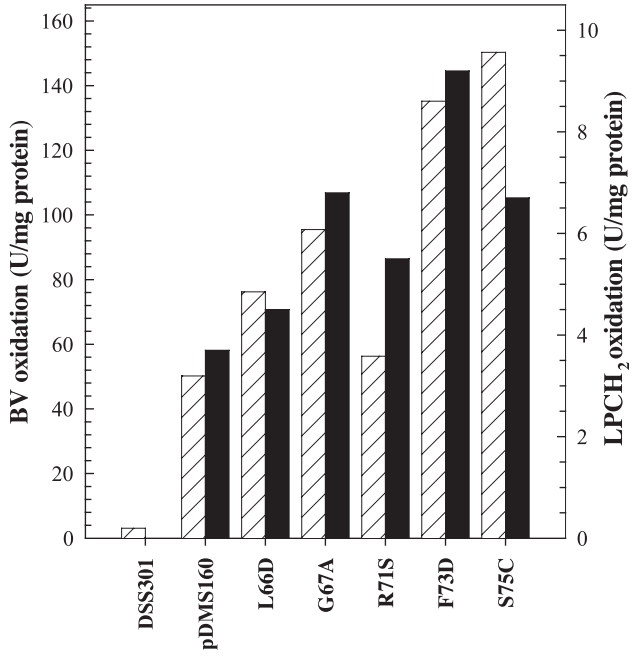

Fig. 2. BV- and $LPCH_2$-mediated activities in membranes prepared from *E. coli* DSS301 harboring pDMS160 plasmids which express DMSO reductase with DmsC-L66D, G67A, R71S, F73D and S75C mutants. Assays were carried out as described in Materials and methods. The left axis and white bars represent the specific BV activity. The right axis and black bars represent the specific $LPCH_2$ activity.

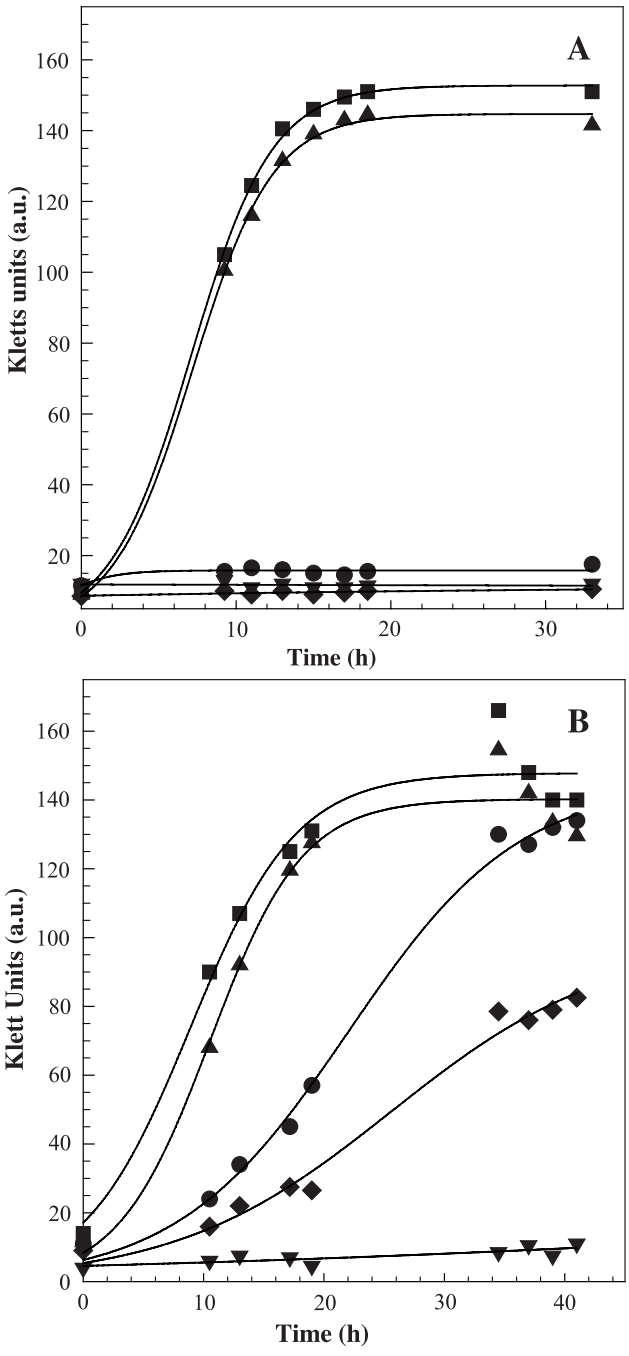

Fig. 3. Anaerobic growth on glycerol/DMSO minimal media of *E. coli* harboring plasmids which express DMSO reductase with DmsC mutants of the glutamate 87 residue. (A) Growth of *E. coli* DSS301 harboring plasmids which express DMSO reductase with DmsC mutants. (B) Growth of *E. coli* HB101 harboring plasmids which express DMSO reductase with DmsC mutants. Symbols: (●) host, (■) wild-type pDMS160, (▲) pDMS160$^{DmsC\text{-}E87D}$, (▼) pDMS160$^{DmsC\text{-}E87K}$, (◆) pDMS160$^{DmsC\text{-}E87Q}$.

Membranes were prepared from DSS301 cells harboring plasmids with the five different mutations. We investigated

the effect of the introduced mutations in DmsC on both the BV- and $LPCH_2$-mediated TMAO reduction activity. BV-mediated TMAO reduction assays the functionality of the catalytic DmsA-subunit because BV donates electrons to DMSO reductase at an unknown site, independent of the menaquinol binding site. The quinol analogue, $LPCH_2$, has previously been shown to be a useful substrate for DMSO reductase to assay electron transfer from the quinol binding site to DmsA [18]. In Fig. 2, the BV and $LPCH_2$ activities are shown for DSS301 (Δ*dmsABC*). DSS301 has no $LPCH_2$ activity as expected since it lacks DMSO reductase. The very low BV activity observed for the host (DSS301) represents residual periplasmic TMAO reductase that has co-purified with the membrane vesicles. The BV and $LPCH_2$ activities vary about 2-fold and this was consistent with the expression level of DMSO reductase in the preparations as analysed by SDS-PAGE and molybdenum cofactor (Form A) content (data not shown). A comparison of the BV/$LPCH_2$ activity ratios can be made between the mutants and pDMS160. The ratio for pDMS160 is 14 and the mutants have ratios of 17, 14, 10, 15 and 23 for the $pDMS160^{DmsC\text{-}L66D}$, $pDMS160^{DmsC\text{-}G67A}$, $pDMS160^{DmsC\text{-}R71S}$, $pDMS160^{DmsC\text{-}F73D}$ and $pDMS160^{DmsC\text{-}S75C}$, respectively. The variation in the ratio between the mutant plasmids and pDMS160 is not significant and it was concluded that the mutations introduced in the loop between helix two and three had no effect on activity or assembly of DMSO reductase.

3.2. Mutagenesis of glutamate 87 on the periplasmic side of helix three of DmsC

Glutamate 87 is located close to the periplasmic side of helix three based on topology determinations [12] and is conserved in all six homologues of DmsC (Fig. 1B). Site-directed mutants of E87 to aspartate, lysine or glutamine were incorporated into DmsC and verified by DNA sequencing. The mutants were characterised by the ability of plasmids expressing the mutant enzymes to complement the anaerobic growth of DSS301 (lacking chromosomally expressed DMSO reductase) and HB101 on glycerol/DMSO minimal media (Fig. 3). The plasmids $pDMS160^{DmsC\text{-}E87K}$ and $pDMS160^{DmsC\text{-}E87Q}$ were unable to complement growth in DSS301 whereas the $pDMS160^{DmsC\text{-}E87D}$ mutant grew as well as DSS301/pDMS160 cells (wild-type) (Fig. 3A). In HB101 cells, the $pDMS160^{DmsC\text{-}E87K}$ mutant showed a dominant negative suppression of growth (Fig. 3B) presumably due to the excess plasmid-encoded mutant enzyme displacing the wild-type chromosomal enzyme from the membrane. The enzyme expressed from $pDMS160^{DmsC\text{-}E87Q}$ could support growth in HB101 but at a rate slower than the wild-type and the $pDMS160^{DmsC\text{-}E87D}$ mutant behaved as enzyme expressed from pDMS160. The doubling times of anaerobic growth on glycerol/DMSO minimal media for the mutants were 4.1 h for both the pDMS160 and $pDMS160^{DmsC\text{-}E87D}$ in DSS301. In HB101, the doubling times were 11.8, 7.3, 7.0 and 11.2 h for the host, $pDMS160^{wt}$, $pDMS160^{DmsC\text{-}E87D}$ and $pDMS160^{DmsC\text{-}E87Q}$, respectively.

The inability of the lysine and glutamine mutants to complement anaerobic growth on glycerol/DMSO media in DSS301 could be due to impaired assembly or loss of electron transfer from DmsC to DmsB. To investigate assembly, membranes were prepared from DSS301 cells harboring the appropriate plasmids and analysed on SDS-PAGE (Fig. 4, left). The expression levels were also verified with Western blotting with polyclonal DmsA and DmsB antibodies (Fig. 4, right). Both the DmsA and DmsC bands are clearly visible in all three mutants. DMSO reductase was also expressed well in membranes from the HB101 cells as judged by the SDS-PAGE (data not shown).

The Mo-bisMGD content associated with the membranes can be estimated with the Form A assay [19]. The assay gives a relative estimate on the amount of DmsA associated with the membrane. The Form A assay of the mutant enzymes expressed in DSS301 membranes confirms the results from the SDS-PAGE. In DSS301, the amount of

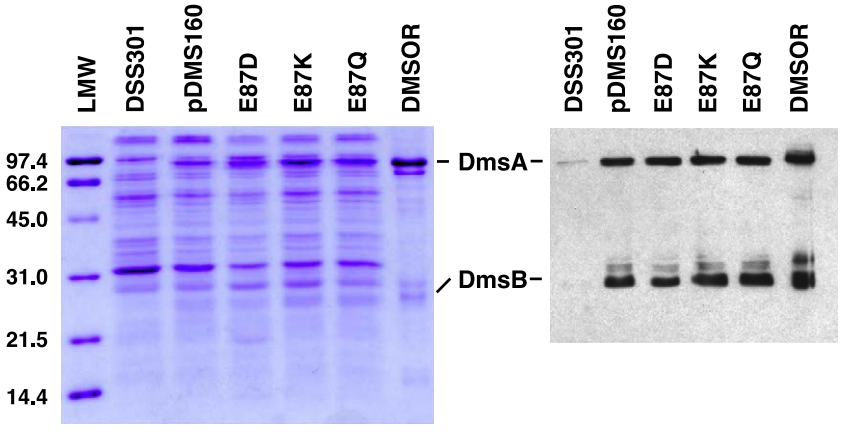

Fig. 4. SDS-PAGE and Western blot of membranes prepared from *E. coli* DSS301 harboring plasmids which express DMSO reductase with DmsC mutants. The membranes are loaded on the gel at 10 μg protein per lane. DmsA has a molecular weight of 85.8 kDa and DmsB of 22.7 kDa. DmsC cannot be detected with Coomassie brilliant blue due to its hydrophobicity. DMSOR—purified DmsAB proteins.

Form A in all three mutants is 25–47% higher than pDMS160 (Table 1). In HB101, the Form A assay shows that there is the same amount of the molybdenum cofactor per milligram of protein in the enzyme expressed from pDMS160$^{DmsC-E87D}$ and the pDMS160$^{DmsC-E87Q}$ mutants as for pDMS160 (Table 2). The enzyme expression from pDMS160$^{DmsC-E87K}$ is slightly lower; however, in all cases the mutant plasmids supported reasonable levels of enzyme expression confirming that the inability to complement growth was not due to impaired assembly of DMSO reductase on the membrane.

The specific activities of the BV and $LPCH_2$ activities for the membranes prepared from DSS301 and HB101 are presented in Tables 1 and 2, respectively. The specific BV activities for membranes containing the aspartate, lysine or glutamine mutant DMSO reductase were close to the values observed for overexpressed wild-type DMSO reductase. The specific $LPCH_2$ activities differed significantly comparing the E87K and E87Q mutant containing membranes to the wild-type and the E87D mutant. The E87K and E87Q mutant enzymes were unable to oxidise $LPCH_2$, whereas the E87D enzyme retained wild-type oxidation levels in both DSS301 and HB101. The ratio between BV and $LPCH_2$ oxidation is a good indicator of the functionality of DMSO reductase. For wild-type enzyme, the ratio is approximately 15 in membranes from both HB101 and DSS301. In the DSS301 membranes, the ratios are 12, 334 and 91 for the E87D, E87K and E87Q, respectively (Table 1). The ratios for DMSO reductase activity in HB101 membranes containing the E87D, E87K and E87Q enzymes are 18, 135 and 116, respectively (Table 2). We determined the K_m and V_{max} of DMSO reductase for $LPCH_2$ in membranes isolated from cells expressing DSSS301/pDMS160 and DSS301/pDMS160$^{DmsC-E87D}$. The specific activities of the E87K and E87Q enzyme-containing membranes were too low for K_m determination. The K_m for the pDMS160$^{DmsC-E87D}$ membranes was 151 μM compared to 168 μM for wild-type DMSO reductase. The activity assays confirmed that menaquinol oxidation is impaired by the insertion of a lysine or a glutamine in place of E87 in DmsC, whereas an aspartate substitution has no effect.

HOQNO is a potent inhibitor of menaquinol binding in DMSO reductase. The K_d for HOQNO binding to wild-type DMSO reductase has been determined by stopped-flow measurements to be 6 nM [9]. We measured the HOQNO binding using a fluorescence quench titration method for membranes containing all three E87

Table 1
Characterisation of DMSO reductase in the different glutamate 87 mutants from the DSS301 strains

Mutants	BV (μmol/(mg prot × min))	$LPCH_2$ (μmol/(mg prot × min))	BV/$LPCH_2$ ratio	Form A (a.u.)	K_m (μM)	V_{max} (μmol/(mg prot × min))
DSS301	3.1	0	–	0	n.d.[a]	n.d.
pDMS160	50.2	3.7	14	1.0	168	11
E87D	81.6	7.0	12	1.47	151	10.1
E87K	66.8	0.20	334	1.27	n.d.	n.d.
E87Q	59.1	0.65	91	1.27	n.d.	n.d.

The specific activities for BV- and $LPCH_2$-mediated TMAO reduction. Determination of the amount of Mo-bisMGD cofactor associated to the membrane are given as relative numbers with the DSS301 host strain representing 0 and overexpressed wild-type 1.

[a] n.d.—not determined.

Table 2
Characterisation of DMSO reductase in the different glutamate 87 mutants from the HB101 strains

Mutants	BV (μmol/(mg prot × min))	$LPCH_2$ (μmol/(mg prot × min))	BV/$LPCH_2$ ratio	Form A (a.u.)	K_d (HOQNO) (nM)
HB101	14.0	0.87	16	0	10.2
pDMS160	74.7	5.6	13	1.0	7.1
E87D	107.2	6.1	18	1.02	8.1
E87K	62.0	0.46	135	0.68	250–400
E87Q	76.5	0.66	116	1.0	33.0

The specific activities for BV- and $LPCH_2$-mediated TMAO reduction. Determination of the amount of Mo-bisMGD cofactor associated to the membrane are given as relative numbers with the HB101 host strain representing 0 and overexpressed wild-type 1. HOQNO inhibition binding was studied in HB101 membranes to minimise the presence of background HOQNO binding.

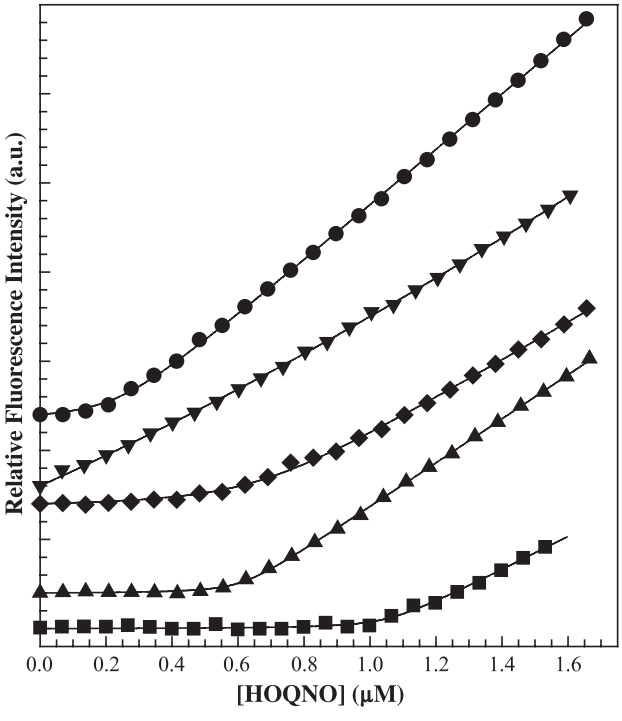

Fig. 5. HOQNO Fluorescence quench titration of membranes prepared from *E. coli* HB101 harboring plasmids which express DMSO reductase with DmsC glutamate 87 mutants. HOQNO binding was measured at 1.0 mg protein per ml. Symbols: (●) host, (■) wild-type pDMS160, (▲) pDMS160$^{DmsC-E87D}$, (▼) pDMS160$^{DmsC-E87K}$, (♦) pDMS160$^{DmsC-E87Q}$.

mutants and compared the binding to wild-type enzyme. Membranes isolated from DSS301 cells were unsuitable for this assay due to very high background binding from fumarate reductase in this strain [14]. In Fig. 5, the binding curves for HB101 membranes expressing chromosomal DMSO reductase, the DMSO reductase expressed by pDMS160 and the three mutants at 1 mg protein per ml are shown. HOQNO binds with high affinity to the control membranes with chromosomal DMSO reductase, membranes expressing pDMS160 DMSO reductase and membranes expressing pDMS160$^{DmsC\text{-}E87D}$ as indicated by the sharp curvature of the binding curve. The binding curve of membranes isolated from HB101/pDMS160$^{DmsC\text{-}E87Q}$ has a more gradual curvature indicative of a decreased binding affinity for HOQNO. The DMSO reductase in membranes isolated from HB101/pDMS160$^{DmsC\text{-}E87K}$ showed very weak HOQNO binding with a slight curvature. The K_d for HOQNO binding in the membranes isolated from HB101/pDMS160$^{DmsC\text{-}E87D}$ is slightly higher than that for pDMS160 (8.1 vs. 7.1 nM) but this is within the experimental error of the technique (Table 2). Membranes isolated from HB101/pDMS160$^{DmsC\text{-}E87Q}$ have a K_d of 33 nM, approximately 4.5 times higher than wild-type and the HB101/pDMS160$^{DmsC\text{-}E87K}$ mutant has a K_d between 250 and 400 nM. The very low affinity makes an exact determination of the K_d difficult.

4. Discussion

The structure of *E. coli* DMSO reductase has not been solved and there is only a proposed topology of DmsC [12]. DmsC provides both the anchor for DmsAB and the menaquinol binding/oxidation site. In this study, we focused on amino acids in the loop between helices two and three that could participate in menaquinol binding and oxidation. Previous work has shown that mutation of histidine 65 to arginine abolishes menaquinol binding and the function of DMSO reductase [8]. This residue is located at the end of helix two, N-terminal to the region chosen for this study. This region is highly conserved between six different sequences of DmsC from *E. coli*, *S. typhimurium* (DmsC-1 and DmsC-2), *H. influenzae*, *Y. pestis* and YnfH from *E. coli* (Fig. 1).

We mutated leucine 66, glycine 67, arginine 71, phenylalanine 73, serine 75 and glutamate 87. Our study shows that mutation of most of the selected conserved residues located in the loop between helices two and three had no effect on assembly or menaquinol oxidation. Only mutation of glutamate 87 to lysine or glutamine abolished growth on glycerol/DMSO minimal media and prevented menaquinol oxidation in DMSO reductase. This residue is proposed to be located at the beginning of helix three on the periplasmic side of the membrane [12].

There are no strong sequence-motifs identified for menaquinol binding sites although weak sequence motifs have been identified for ubiquinone binding proteins [22]. However, a growing number of high-resolution structures of menaquinol binding enzymes are becoming available in the Protein Data Bank. The menaquinol binding site is composed of the three-dimensional organisation of hydrophobic and polar residues drawn from adjacent helices and loops. One structure that is useful for comparison with the membrane anchor of DMSO reductase is fumarate reductase from *E. coli*. Both enzymes utilise menaquinol and lack hemes in the menaquinol binding membrane anchor. Succinate dehydrogenase, formate dehydrogenase and nitrate reductase all contain heme at the quinol binding sites in the membrane anchors [23–25] and we chose not to use them for our comparison. Fumarate reductase from *E. coli* has been studied thoroughly (see Ref. [26] for further references). Only a small number of amino acid residues in the structure of FrdABCD define the menaquinol binding site. In fumarate reductase, the menaquinol binding pocket is lined by histidine, arginine, glutamate, phenylalanine and tryptophane from helices one and two in both FrdC and FrdD. Identifying corresponding amino acids in DmsC could increase the understanding of how DmsC folds in the membrane. However, it is difficult to identify the menaquinol binding residues in DmsC by examination of conserved residues because the high sequence identity between the *dmsC* genes of different organisms prevents us from identifying a limited number of key residues.

Mutation of FrdC–His82 to arginine abolishes menaquinol oxidation and HOQNO binding but does not alter the assembly, BV activity or the electron paramagnetic resonance signal of the iron–sulfur cluster of fumarate reductase close to the menaquinol binding site. Mutation of DmsC–His65 mimics the FrdC–His82 mutation [27–29]. His82 of fumarate reductase is not involved directly in menaquinol oxidation but contributes to the hydrogen bonding network for other residues in the menaquinol binding site of FrdC (pdb-entry 1FUM, [30]).

Assuming the same function for DmsC–His65, we hypothesized that DmsC–Leu66 and DmsC–Gly67, located downstream from DmsC–His65, and in the periplasmic loop between helices two and three would modify the binding or access of menaquinol into the binding site by introducing bulkier or polar residues. These amino acids were replaced with either aspartate or alanine. Aspartate is comparable in size to leucine but negatively charged and alanine has a larger head group than glycine but maintains the non-polar character. However, no effect of the DmsC–Leu66Asp or DmsC–Gly67Ala mutations was observed.

To date no residues in the loops of FrdC and FrdD have been identified as important for menaquinol binding. However, the membrane-spanning regions of FrdC and FrdD in the crystal structure were slightly shifted from the proposed topology [31,32], and it was important to investigate the loop regions in the hypothetical DmsC topology. We made site-

directed mutants of three additional conserved residues proposed to be in the periplasmic loop between helix two and three. We studied mutations in DmsC–Arg71, DmsC–Phe73 and DmsC–Ser75 to serine, aspartate and cysteine, respectively. We could not observe any physiologic effect of the mutations and we conclude that the loop between helix two and three in DmsC is not important for menaquinol binding.

In this paper, we show that DmsC–Glu87 is important for menaquinol binding and HOQNO binding. When DmsC–Glu87 was replaced with glutamine, the ability to grow on glycerol/DMSO minimal media was lost. The binding of HOQNO was also affected. The negative charge of the glutamate is important for correct binding of menaquinol and the quinol inhibitor but the menaquinol binding site is not sterically restricted, as the smaller aspartate can substitute for DmsC–Glu87 without any loss of function. A larger, positively charged amino acid (lysine) completely abolished menaquinol oxidation and binding of HOQNO. This is again similar to fumarate reductase where FrdC–Glu29 in helix one was important for menaquinol oxidation and HOQNO binding. Glutamate has been shown to be important for menaquinol binding in several enzymes such as fumarate reductase both from *E. coli* and *W. succinogenes* as well as other enzymes [26,32,33]. The glutamate probably acts as a Lewis acid and Bronstead base for a proton from menaquinol.

Two residues have now been identified as important for menaquinol binding in DMSO reductase. Mutation of either DmsC–His65 or DmsC–Glu87 abolished the ability to grow on glycerol/DMSO minimal media. Although there are no identified sequence motifs for menaquinol binding, an emerging theme can be observed. Histidine and glutamate are important for menaquinol oxidation. These residues are located on the same side of the membrane but not in the same transmembrane helices. There are also aromatic residues sandwiched between the aromatic plane and the isoprenoid chain of menaquinol in published structures of quinol binding proteins. Likely, there will also be important aromatic residues in the menaquinol binding pocket of DmsC.

Acknowledgements

PG is the recipient of a postdoctoral fellowship from the Swedish Foundation for International Cooperation in Research and Higher Education (STINT). The work was supported by grants from the Canadian Institutes of Health Research, the Human Frontier Science Program Organisation and the Alberta Heritage Foundation for Medical Research. The authors would like to acknowledge the summer students John Staples, Indraneal Chatterjee and Norris Wong for the initial characterisation of the E87K and E87Q mutants.

References

[1] J.H. Weiner, R.A. Rothery, D. Sambasivarao, C. Trieber, Molecular analysis of dimethylsulfoxide reductase: a complex iron–sulfur molybdoenzyme of *Escherichia coli*, Biochim. Biophys. Acta 1102 (1992) 1–18.
[2] P.T. Bilous, J.H. Weiner, Molecular cloning and expression of the *Escherichia coli* DMSO reductase operon, J. Bacteriol. 170 (1988) 1511–1518.
[3] P.T. Bilous, S.T. Cole, W.F. Anderson, J.H. Weiner, Nucleotide sequence of the *dmsABC* operon encoding the anaerobic dimethylsulfoxide reductase of *Escherichia coli*, Mol. Microbiol. 2 (1988) 785–795.
[4] J.L. Simala Grant, J.H. Weiner, Kinetic analysis and substrate specificity of *Escherichia coli* dimethyl sulfoxide reductase, Microbiology 142 (1996) 3231–3239.
[5] P.T. Bilous, J.H. Weiner, Dimethyl sulfoxide reductase activity by anaerobically grown *Escherichia coli* HB101, J. Bacteriol. 162 (1985) 1151–1155.
[6] R.A. Rothery, J.L. Simala Grant, J.L. Johnson, K.V. Rajagopalan, J.H. Weiner, Association of molybdopterin guanine dinucleotide with *Escherichia coli* dimethyl sulfoxide reductase: effect of tungstate and a mob mutation, J. Bacteriol. 177 (1995) 2057–2063.
[7] R. Cammack, J.H. Weiner, Electron paramagnetic resonance spectroscopic characterization of DMSO reductase of *Escherichia coli*, Biochemistry 29 (1990) 8410–8416.
[8] R.A. Rothery, J.H. Weiner, Interaction of an engineered [3Fe–4S] cluster with a menaquinol binding site of *Escherichia coli* DMSO reductase, Biochemistry 35 (1996) 3247–3257.
[9] Z. Zhao, J.H. Weiner, Interaction of 2-*n*-heptyl-4-hydroxyquinoline-*N*-oxide with dimethyl sulfoxide reductases of *Escherichia coli*, J. Biol. Chem. 273 (1998) 20758–20763.
[10] R.A. Rothery, C. Trieber, J.H. Weiner, Interactions between the molybdenum cofactor and iron–sulfur cluster of *Escherichia coli* dimethylsulfoxide reductase, J. Biol. Chem. 274 (1999) 13002–13009.
[11] D. Sambasivarao, J.H. Weiner, Dimethyl sulfoxide reductase of *Escherichia coli*: an investigation of function and assembly by use of in vivo complementation, J. Bacteriol. 173 (1991) 5935–5943.
[12] J.H. Weiner, G.M. Shaw, R.J. Turner, C. Trieber, The topology of the anchor subunit of dimethyl sulfoxide reductase of *Escherichia coli*, J. Biol. Chem. 268 (1993) 3238–3244.
[13] J. Sambrook, D.W. Russel, Molecular Cloning: A Laboratory Manual, Cold Spring Harbor Laboratory Press, Cold Spring Harbor, NY, 2001.
[14] R.A. Rothery, J.H. Weiner, Alteration of the iron–sulfur cluster composition of *Escherichia coli* dimethyl sulfoxide reductase by site-directed mutagenesis, Biochemistry 30 (1991) 8296–8305.
[15] U.K. Laemmli, Cleavage of structural proteins during the assembly of the head of bacteriophage T4, Nature 227 (1970) 680–685.
[16] D. Sambasivarao, D.G. Scraba, C. Trieber, J.H. Weiner, Organization of dimethyl sulfoxide reductase in the plasma membrane of *Escherichia coli*, J. Bacteriol. 172 (1990) 5938–5948.
[17] R.W. Jones, P.B. Garland, Sites and specificity of the reaction of bipyridylium compounds with anaerobic respiratory enzymes of *Escherichia coli*. Effects of permeability barriers imposed by the cytoplasmic membrane, Biochem. J. 164 (1977) 199–211.
[18] R.A. Rothery, I. Chatterjee, G. Kiema, M.T. McDermott, J.H. Weiner, Hydroxylated naphtoquinones as substrates for *Escherichia coli* anaerobic reductases, Biochem. J. 332 (1998) 34–41.
[19] J.L. Johnson, K.V. Rajagopalan, Structural and metabolic relationship between the molybdenum cofactor and urothione, Proc. Natl. Acad. Sci. U. S. A. 79 (1982) 6856–6860.
[20] G. van Ark, J.A. Berden, Binding of HOQNO to beef-heart sub-mitochondrial particles, Biochim. Biophys. Acta 459 (1977) 119–127.
[21] J.G. Okun, P. Lümmen, U. Brandt, Three classes of inhibition share a common binding domain in mitochondrial complex I (NADH:ubiquinone oxidoreductase), J. Biol. Chem. 274 (1999) 2625–2630.

[22] P. Rich, N. Fisher, Generic features of quinone-binding sites, Biochem. Soc. Trans. 27 (1999) 561–565.
[23] V. Yankovskaya, R. Horsefield, S. Tornroth, C. Luna-Chavez, H. Miyoshi, C. Leger, B. Byrne, G. Cecchini, S. Iwata, Architecture of succinate dehydrogenase and reactive oxygen species generation, Science 299 (2003) 700–704.
[24] M. Jormakka, S. Tornroth, B. Byrne, S. Iwata, Molecular basis of proton motive force generation: structure of formate dehydrogenase-N, Science 295 (2002) 1863–1868.
[25] M.G. Bertero, R.A. Rothery, M. Palak, C. Hou, D. Lim, F. Blasco, J.H. Weiner, N.C.J. Strynadka, Insights into the respiratory electron transfer pathway from the structure of nitrate reductase A, Nat. Struct. Biol. 10 (2003) 681–687.
[26] G. Cecchini, I. Schröder, R.P. Gunsalus, E. Maklashina, Succinate dehydrogenase and fumarate reductase from *Escherichia coli*, Biochim. Biophys. Acta 1553 (2002) 140–157.
[27] J.H. Weiner, R. Cammack, S.T. Cole, C. Condon, N. Honore, B.D. Lemire, G.M. Shaw, A mutant of *Escherichia coli* fumarate reductase decoupled from electron transport, Proc. Natl. Acad. Sci. U. S. A. 83 (1986) 2056–2060.
[28] D.J. Westenberg, R.P. Gunsalus, B.A. Ackrell, G. Cecchini, Electron transfer from menaquinol to fumarate. Fumarate reductase anchor polypeptide mutants of *Escherichia coli*, J. Biol. Chem. 265 (1990) 19560–19567.
[29] R.A. Rothery, J.H. Weiner, Interaction of a menaquinol binding site with the [3Fe–4S] cluster of *Escherichia coli* fumarate reductase, Eur. J. Biochem. 254 (1998) 588–595.
[30] T.M. Iverson, C. Luna-Chavez, G. Cecchini, D.C. Rees, Structure of the *Escherichia coli* fumarate reductase respiratory complex, Science 284 (1999) 1961–1966.
[31] T.M. Iverson, C. Luna-Chavez, L.R. Croal, G. Cecchini, D.C. Rees, Crystallographic studies of the *Escherichia coli* quinol-fumarate reductase with inhibitors bound to the quinol-binding site, J. Biol. Chem. 277 (2002) 16124–16130.
[32] D.J. Westenberg, R.P. Gunsalus, B.A. Ackrell, H. Sices, G. Cecchini, *Escherichia coli* fumarate reductase *frdC* and *frdD* mutants. Identification of amino acid residues involved in catalytic activity with quinones, J. Biol. Chem. 268 (1993) 815–822.
[33] C.R.D. Lancaster, R. Gross, A. Haas, M. Ritter, W. Mantele, J. Simon, A. Kroger, Essential role of Glu-C66 for menaquinol oxidation indicates transmembrane electrochemical potential generation by *Wolinella succinogenes* fumarate reductase, Proc. Natl. Acad. Sci. U. S. A. 97 (2000) 13051–13056.